Journal of Medicinal Chemistry

ACS AuthorChoice

Article

pubs.acs.org/jmc

Terms of Use

An Allosteric Modulator of HIV-1 Protease Shows Equipotent Inhibition of Wild-Type and Drug-Resistant Proteases

Peter M.-U. Ung,[†] James B. Dunbar, Jr.,[†] Jason E. Gestwicki,[‡] and Heather A. Carlson*[,†]

[†]Department of Medicinal Chemistry, College of Pharmacy, University of Michigan, 428 Church Street, Ann Arbor, Michigan 48109-1065, United States

[‡]Department of Pathology and the Life Sciences Institute, University of Michigan, 210 Washtenaw Avenue, Ann Arbor, Michigan 48109-2216, United States

Supporting Information

ABSTRACT: NMR and MD simulations have demonstrated that the flaps of HIV-1 protease (HIV-1p) adopt a range of conformations that are coupled with its enzymatic activity. Previously, a model was created for an allosteric site located between the flap and the core of HIV-1p, called the Eye site (*Biopolymers* **2008**, *89*, 643−652). Here, results from our first study were combined with a ligand-based, lead-hopping method to identify a novel compound (NIT). NIT inhibits HIV-1p, independent of the presence of an active-site inhibitor such as pepstatin A. Assays showed that NIT acts on an allosteric site other than the dimerization interface. MD simulations of the ligand−protein complex show that NIT stably binds in the Eye site and restricts the flaps. That bound state of NIT is consistent with a crystal structure of similar fragments bound in the Eye site (*Chem. Biol. Drug Des.* **2010**, *75*, 257−268). Most importantly, NIT is equally potent against wild-type and a multidrug-resistant mutant of HIV-1p, which highlights the promise of allosteric inhibitors circumventing existing clinical resistance.

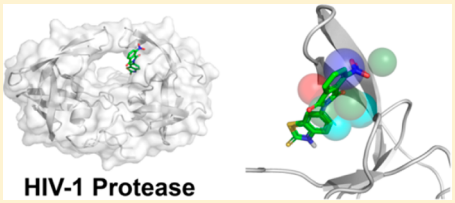

INTRODUCTION

Proteins are inherently dynamic and conformationally heterogeneous. It is generally recognized that they exist in an ensemble of differently populated conformational states in equilibrium, where certain conformations play crucial roles in protein functions such as enzymatic activity and molecular recognition.[3,4] Therefore, it may be possible to design ligands that specifically target certain conformational states of a protein and "lock" it into an inactive state.[5−8]

The aforementioned phenomenon can also be applied to other protein systems to modulate enzymatic activity. In this study, we focus on the clinically important HIV-1 protease (HIV-1p). HIV-1p is a C_2-symmetric, homodimeric protease (Figure 1A). It is critical in the maturation of the infective HIV virion[9] as it cleaves the *gag* and *gag-pol* polyproteins to release the structural proteins (MA, CA, NC, and p6) and the enzymes reverse transcriptase, integrase, and protease.[10] Thus, it is an important target for HIV infection treatments and has led to several FDA-approved drugs that specifically target its active site, which catalyzes the hydrolysis of the substrate peptides.

The active site of HIV-1p is gated by a pair of glycine-rich, β-hairpin loops, one from each monomeric HIV-1p, which is commonly referred to as the "flaps" (K45-M-I-G-G-I-G-G-F-I54). The flaps control the access and positioning of the substrate in the active site during hydrolysis, thus their mobility is essential to HIV-1p activity. Several studies based on crystallography,[11,12] EPR,[13,14] NMR,[15] and molecular dynamics (MD) simulations[16−18] suggest that the flaps of HIV-1p exist in an ensemble of conformational states and can adopt a range of conformations (closed, semiopen, and open).[19−22]

HIV-1p possesses hydrophobic flap-tip recognition pockets, or "Eye" sites, consisting of residues Val32, Ile47, Gly48, Gly49, Ile50, Ile54, Val56, Gly78, Pro79, Thr80, Pro81, and Ile84 (Figure 1A). Upon substrate binding, each flap closes down and positions its flap tip (residues 49−52) into this highly conserved region on the opposite-side monomer. These sites are not present in the closed form as the flap tip of the opposing monomer occupies each site. However, in the event of flap opening, the flap tip undocks and the flap handedness reverses, opening up the Eye site.

As the opening of the Eye site is dependent upon the positions of the flaps, we previously hypothesized that specifically targeting this Eye site with the binding of a small molecule could modulate the enzymatic activity of the protease through altering the dynamics of the flaps and the equilibrium of the flap conformational states.[1] To identify such inhibitors, the varied conformations of the flaps were used to create a pharmacophore model of the Eye site that was used for virtual screening. This novel Eye-site pharmacophore model was constructed using the multiple protein structures (MPS) method[23−26] (Figure 1B). Our earlier study screened the Center of Chemical Genomics (CCG) library against the Eye site pharmacophore model, and subsequent testing of the computational hits identified compound **1** as our best inhibitor of HIV-1p proteolytic activity (Figure 1C).

The possibility of targeting the Eye site was confirmed by a recent study by Perryman et al.[2] that identified potential

Received: March 26, 2014
Published: July 25, 2014

   dx.doi.org/10.1021/jm5008352 | *J. Med. Chem.* 2014, 57, 6468−6478

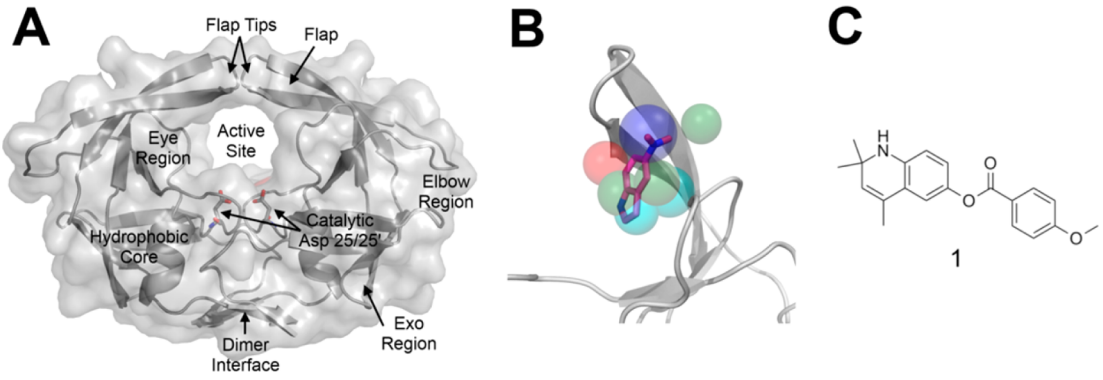

Figure 1. (A) Cartoon representation of HIV-1p in the semiopen conformation (PDB: 1HHP). (B) Pharmacophore model of the HIV-1p allosteric site, the Eye site, constructed by Damm et al.[1] When the 5NI–protease crystal structure is superimposed on the pharmacophore model, the agreement is obvious. The pharmacophores are color-coded according to chemical property: hydrophobic (cyan), aromatic (green), hydrogen-bond donor (red), and hydrogen-bond acceptor (blue). (C) Structure of compound **1** with inhibitory activity against HIV-1p.

allosteric sites of HIV-1p through fragment-based crystallography. Of particular interest was a 2.1 Å crystal of fragment-bound HIV-1p in semiopen conformation because the molecular probe 5-nitroindole (5NI) was found to reside in the Eye site of HIV-1p. In this particular 5NI-bound HIV-1p crystal structure, the molecular probe 5NI forms hydrophobic contacts with Val32, Ile47, Ile54, Pro81, and Ile84, and a hydrogen bond with the Gly51 amide through 5NI's nitro group. These residues have been suggested to play a role in flap recognition.[16] This is the first crystallographic confirmation that demonstrates the existence of the Eye site in the semiopen HIV-1p, supporting the notion that the Eye site is a viable site for small molecule targeting. Furthermore, 5NI fits well within our Eye-site pharmacophore model (Figure 1B) and overlaps with two of the three aromatic pharmacophore elements as well as the hydrogen-bond acceptor element. Furthermore, the crystal structure exhibited ligand binding to only one Eye site, not both, which is consistent with our previous modeling work.[1]

Here, we demonstrate that a nitro-containing compound (NIT) derived from a ligand-based Markush search, which has similarity to 5NI, can modulate the activity of HIV-1p. Additional experimental and computational studies of the nitro-containing ligand suggest it acts through the Eye site, an allosteric site of HIV-1p. Furthermore, it is equipotent against a multidrug resistant (MDR) HIV-1p, which shows that inhibitors with this mode of action can overcome existing clinical resistance. Although NIT has only lead-like affinity, its small size (MW = 357) gives a respectable ligand efficiency of −0.23 kcal/mol·heavy-atom. It is the first small, drug-like molecule to be fully characterized as having an alternative mechanism against HIV-1p and the ability to evade existing clinical resistance.

MATERIALS AND METHODS

Markush Chemical-Similarity Search. UNITY,[27,28] a module of the SYBYL[29] suite (version 8.0), was used for ligand-based chemical search. A Markush search was constructed based on the chemical structure and connectivity of the reference structure, compound **1**. UNITY performed the query searches against academic and commercial chemical libraries: ChemBridge (2007), ChemDiv (2007), MayBridge (2007), and the CCG (2007.10) chemical libraries. Compounds that matched the queries were selected, and 3D comparisons to compound **1** were used to further prioritize the sets. The 3D conformers were generated with OMEGA 2.3.2,[30] a module of the OpenEye suite. The selected compounds were scored and ranked by ROCS (version 3.0.0) and EON (version 2.0.1), respectively.[31] ROCS scores a chemical according to its shape similarity to the bound pose from our previous work,[1] while EON scores the charge distribution similarity of a chemical to the reference structure. A consensus score of the ROCS and EON scores with equal weight were used to rank the selected compounds. The top 200 compounds from each library were examined manually, and 48 compounds were selected for testing experimentally based on diversity, size, solubility, cost, and availability from the vendors (CCG, 5 compounds; ChemBridge, 30 compounds; ChemDiv, 8 compounds; MayBridge, 5 compounds).

Inhibitor Screening Assay. Pseudo wild-type (WT; G7K) and a MDR strain (L10I/L63P/A71V/G73S/I84V/L90M) of HIV-1p were kindly provided by Dr. Celia Schiffer of the University of Massachusetts. Pseudo-WT protease was used to avoid autoproteolysis activity of HIV-1p. A resonance energy transfer (FRET)-based biochemical assay was used to assess the HIV-1p enzymatic activity. A fluorogenic peptide substrate was used, RE(EDANS)SQNYPIVQK-(Dabcyl)R (Molecular Probes, Catalogue no. H-2930) was used. This substrate contains a fluorophore EDANS and a chromophore Dabcyl, which quenches the excited fluorophore when the two chromophores are in close proximity.[32] EDANS has an excitation wavelength near 340 nm and emission wavelength near 490 nm, while Dabcyl has an excitation wavelength overlapping the emission range of EDANS. The peptide substrate turnover by the protease was monitored by the spectrometer SpectraMax M5 from the Molecular Devices. Top-read mode was used in the fluorescence detection, where excitation/emission wavelengths of EDANS at 340 and 490 nm, respectively, were monitored. A 475 nm cutoff filter was applied to reduce the noise signal. Screening assays were performed in triplicate in black, round-bottom, low-volume, 384-well plates (Corning no. 3676).

All purchased compounds were screened at 150 μM (HIV-1p at 30 nM and substrate at 2 μM). Stock solution of the tested compound dissolved in DMSO was diluted with milli-Q H_2O to 10-fold the desired final concentration. Final concentration of DMSO in the assay was kept below 2% v/v.[33] Milli-Q H_2O and pepstatin A (PepA) were used as the negative and positive controls, respectively. The ligand solution was mixed with the protease in the standard assay buffer (100 mM sodium acetate, 1 M NaCl, 1 mM EDTA, 1 mM DTT, 20% v/v glycerol, 0.1% w/w CHAPS, 0.2% v/v PEG-400, pH = 4.7)[1,34−38] and incubated for 30 min at room temperature. The enzymatic assay was initiated by introduction of the fluorogenic peptide substrate (diluted in assay buffer) and shaken for 15 s inside the plate reader; the assay was monitored for 10 min at 30 °C. The kinetic data was fitted linearly to determine the rate of fluorogenic substrate turnover, measured as change in fluorescence intensity per unit time. Inhibitory activity was calculated by comparing the turnover rate against the negative control,

dx.doi.org/10.1021/jm5008352 | J. Med. Chem. 2014, 57, 6468−6478

$$\%\text{remaining protease activity} = \left(\left(\frac{d(RFU)_{ligand}}{dt}\right)\Big/\left(\frac{d(RFU)_{negative}}{dt}\right)\right) \times 100\%$$

where RFU is the raw fluorescence unit measured by the spectrometer.

Michaelis–Menten Kinetics. The Michaelis–Menten kinetics of the fluorogenic peptide substrate with WT or MDR HIV-1p was performed by varying the fluorogenic substrate concentration between 2.5 and 100 μM against a constant concentration of HIV-1p at 30 nM. The experimental conditions were identical to those mentioned above. As this experiment requires the use of high concentrations of fluorogenic peptide substrate, which contains the chromophore Dabcyl, reabsorption of the fluorophore-emitted light by the chromophores in the solution will be significant. This effect, called the inner filter effect, will disproportionally affect and reduce the intensity of observed fluorescence at high substrate concentration (>20 μM) while having little influence on the intensity of fluorescence at low substrate concentration. To correct this effect, a standard curve of EDANS fluorescence against an increasing concentration of the fluorogenic peptide substrate was obtained and used to correct the intensity of observed fluorescence. The data-analysis package SigmaPlot version 11.0 (from Systat Software, Inc., San Jose California USA, www.sigmaplot.com) was used to calculate the Michaelis constant (K_m) by fitting the data to an one-site saturation model with a nonlinear regression method.

Dose-Dependent Inhibition Assay. For IC_{50} determination, the final concentrations of protease and fluorogenic peptide substrate were 30 nM and 5 μM, respectively. For our buffer and assay condition, K_m of the substrate was determined to be 91 ± 11 and 207 ± 26 μM for WT and MDR HIV-1p, respectively. IC_{50} and Hill slope were obtained by fitting the kinetic data to a sigmoidal dose–response model using SigmaPlot. Assuming that dose–response kinetics are appropriate to describe allosteric inhibition, the inhibition constant (K_i) of the tested compound was obtained through the Cheng–Pursoff equation

$$K_i = \frac{IC_{50}}{\left(1 + \frac{[S]}{K_m}\right)}$$

Dimerization Inhibition Analysis. To rule out the mechanism where the compounds inhibit dimerization, Zhang–Poorman kinetics analysis was performed.[37,39−41] Protease concentration was varied between 0.5 and 30 nM while substrate concentration was fixed at 10 μM. The kinetic data was plotted as $\sqrt{v_i}$ vs $[E]_0/\sqrt{v_i}$, where v_i is the rate of substrate turnover and $[E]_0$ is the concentration of the protease. The kinetic data was linearly fitted and the mode of inhibition was determined by comparing the slope of the curves, where parallel lines indicate the compound modulates protease activity through binding the monomer and blocking dimerization while intercepting lines indicate the mode of inhibition targets the dimeric form of HIV-1p.

Cross-Competitive Inhibition. A variation of Yonetani–Theorell kinetic analysis was used to examine the mode of inhibition.[42,43] PepA, a known competitive inhibitor for HIV-1p, was used in this kinetic assay. PepA concentration varied from 0–300 nM in assay with WT HIV-1p and 0–400 nM with MDR HIV-1p.[44] The concentrations of substrate and protease were kept at 5 μM and 30 nM, respectively, while other experimental conditions were the same as above. The kinetic data was plotted as v_0/v_i versus $[PepA]/IC_{50PepA}$. The kinetic data was fitted linearly to determine the interaction factor that defines the type of interaction (agonistic, antagonistic, or mutually exclusive) between the known competitive inhibitor and the tested compound.

Dynamics Simulations. Unrestrained all-atom MD and Langevin dynamic (LD) simulations were performed with the FF99SB force field[45] and the AMBER10 suite of programs.[46] An apo HIV-1p in semiopen conformation (PDB: 1HHP[47]) obtained from the PDB[48] was used and the C_2-symmetric homodimer was generated using PyMOL version 1.2.[49] The ionizable groups of the protein were protonated by the defaults in tLEaP and approved through "by hand" inspection. One of the catalytic Asp25s was protonated, from ASP to ASH. The ligand NIT was placed into the Eye site of HIV-1p by docking with Schrödinger's Glide[50] (version 5.5), using standard precision and default settings. The web-based R.E.D.[51] (version 3.4) and Ante_R.E.D. (version 2.0) were used to derive the RESP charge values for the ligand NIT. The ESP charges were determined at HF/6-31G* level with Gaussian09, which were then fitted to the ligand through a two-stage RESP fitting. Force field parameters of NIT were built from analogy to parameters in the general AMBER force field[52] and the RESP charges using the Antechamber module of AMBER.[53]

Five independent, 20 ns MD simulations were performed using different random-number seeds. The NIT–protease complex was solvated with a truncated octahedral TIP3P water box[54] with a buffer distance of 12 Å and closeness parameter of 0.5. The system charge was neutralized with Cl^- counterions. A 10- Å cutoff for van der Waals interactions was used, and particle mesh Ewald for long-range electrostatics[55] was employed. The simulations were run in the NPT ensemble, and SHAKE[56] was used to constrain all bonds to hydrogen atoms to allow a 2 fs time step. To avoid water from inappropriately warping the protein, we applied the following equilibration protocol.[57] For the solvated system, hydrogen atoms were first minimized, followed by the side chains and then all atoms. The system was then equilibrated first with a gradual heating of water from 10 to 310 K over 50 ps and then a water equilibration with protein atoms restrained for 250 ps at 310 K. This was followed by a full system heating from 10 to 310 K over 180 ps and a full system equilibration with protein unrestrained at 310 K for 400 ps. The production phase was run for 20 ns at 310 K.

Five independent, 20 ns LD simulations were also performed. Hydrogen atoms were constrained with SHAKE while a 999 Å cutoff distance for nonbonded interactions was used. Generalized Born approach was used to implicitly model aqueous solvation for the LD simulations.[58] Default dielectric values, where interior = 1 and exterior = 78.5, were used. The time step and the collision frequency of the simulation were 1 fs and 1 ps^{-1}, respectively. Simulations began with hydrogen minimization, followed by side chain and then all-atom minimizations. Equilibration was done in six stages: the system was gradually heated from 100 K to the final temperature at 300 K in the first two equilibration steps. Restraints were placed on all heavy atoms and gradually removed over the first four equilibration steps using force constants from 2.0 to 0.1 kcal/mol·$Å^2$, where the first three steps were done over 10 ps and the fourth step over 50 ps. Only the backbone atoms were restrained at 0.1 kcal/mol·$Å^2$ over 50 ps in the fifth equilibration step. In the sixth equilibration step, the restraints were removed, and all atoms were allowed full freedom for 300 ps at 300 K. The production phase was run for 20 ns. Analysis of the trajectories was performed using the PTRAJ module of AMBER.

Essential Dynamics Analysis. Essential dynamics analysis of the MD trajectory data was used to compare dynamics of the protein structure in simulations.[59,60] PTRAJ was used to perform the orthogonal transformation calculation on the covariance matrix of the backbone heavy atoms and solve for the eigenvectors and the associated eigenvalues of the MD trajectories.[61] The eigenvectors were compared by calculating the dot product of the corresponding vectors in each set of eigenvector. The dot-product values were then rescaled to between 0 and 100, where 0 corresponds to a dot-product of 1.0, i.e., strongly correlated, and 100 corresponds to a dot-product of −1.0, i.e., strongly anticorrelated. The rescaled dot-product values were added to a reference PDB structure for visualization in VMD 1.8.9.[62]

RESULTS AND DISCUSSION

Identification of Compounds through Pharmacophore Screening. The Eye-site pharmacophore model has been used to virtually screen against the CCG library from the University of Michigan. The best inhibitor, 2,2,4-trimethyl-1,2-dihydroquinolin-6-yl 4-methoxybenzoate (compound **1**), had dose-dependent activity against HIV-1p (Figure 1C).[1] This compound was the first experimentally tested, active inhibitor that was designed to target the newly discovered allosteric site rather than the traditional catalytic site.

dx.doi.org/10.1021/jm5008352 | J. Med. Chem. 2014, 57, 6468–6478

The chemistry space around the chemical scaffold of compound **1** was further explored and expanded to identify new scaffolds that would fit the Eye site pharmacophore model and target the allosteric site of HIV-1p. We applied a structure-based, lead-hopping method to explore nearby chemical space. The chemical features of compound **1** were used to generate a Markush chemical similarity search with the following general features: (1) sp^2 N−H connecting to an aromatic ring (analogue to quinolin-6-yl moiety) that can be either a 5- or 6-membered ring, (2) aromatic ring of any decoration (analogue to *p*-methoxy benzoate moiety), and (3) a 3-atom linker of connecting (1) and (2) (analogue to the ester linkage).

The Markush search queries were constructed (Figure 2A) based on the chemical features and connectivity of the

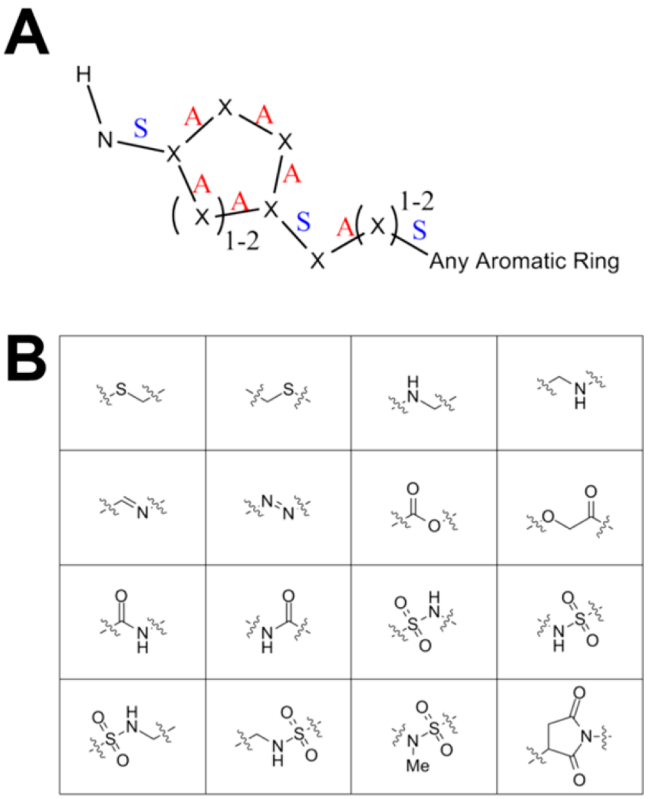

Figure 2. (A) Summary of Markush search based on the chemical features and connectivity of compound **1**. The search queries have these designations: A, any bond order; S, single bond only; x, any heavy atom; *i* and *j*, number of heavy atoms. (B) List of linker moieties used in the filtering of Markush search results.

reference structure, compound **1** (Figure 1C). UNITY, a module of SYBYL suite, was used in the ligand-based chemical search against the CCG library (v2007.10, ∼90000 compounds) and libraries of three commercial vendors: ChemBridge (EXPRESS-Pick v2007, ∼50000 compounds), ChemDiv (2007, ∼120000 compounds), and MayBridge (v2007, ∼56000 compounds) chemical libraries. As a result, 7230 compounds matched the Markush search queries.

To prioritize and rank the compounds that matched the Markush search queries, 3D conformations of the selected compounds were compared to the conformations of compound **1**. The 3D comparisons were scored by ROCS and EON, both modules of the OpenEye suite. ROCS scores a chemical according to its shape complementary to the reference structure (compound **1**), while EON scores based on the similarity of charge distribution of a chemical to the reference structure. A consensus score of the ROCS and EON scores with equal weight were used to rank the selected compounds. The top-200 compounds were examined manually, and only those with fused double aromatic rings (similar to quinolin-6-yl moiety) and unique linkers (Figure 2B) were selected. Finally, 48 compounds (5 from CCG, 30 from ChemBridge, 8 from ChemDiv, and 5 from MayBridge) were purchased for experimental testing (listed in Table S1 of the Supporting Information). One compound, ChemBridge 5979646, was identified to have good inhibitory activity against HIV-1p, and most importantly, it shared chemical features with compound 5NI, the fragment found to bind the Eye site in crystallographic studies.[2] This compound was specifically selected for more in depth study. The mass spectroscopy data and proton NMR spectrum for ChemBridge 5979646 (compound NIT) are given in the Supporting Information, Figure S1. Although nitro groups are often a concern for medicinal chemistry, it is desirable in this case. NIT does not trigger any of the chemical alerts in OpenEye's FILTER[63] program nor does it contain any functional groups identified in the PAINS filter (Pan Assay Interference compounds).[64]

Dose-Dependent Inhibition of NIT. We confirmed that ChemBridge 5979646, 4-nitro-2-(2-thioxo-2,3-dihydrobenzothiazol-6-yl)isoindoline-1,3-dione (NIT, Figure 3A), inhibited WT HIV-1p activity in a dose-dependent manner and has a K_i = 96 ± 3 μM (Figure 3B). This translates into a binding affinity of approximately −5.5 kcal/mol and a respectable binding efficiency of −0.23 kcal/mol·heavy-atom. To eliminate the possibility of NIT as a promiscuous aggregator, we performed a dose-dependence assay at three HIV-1p concentrations (15, 30, 45 nM);[65] no significant change in Hill slope value was observed (Figure 3B, insert).

We investigated the effectiveness of compound NIT against a MDR HIV-1p mutant (L10I/L63P/A71V/G73S/I84V/L90M). Using the competitive inhibitor PepA as the control, we showed that the MDR mutations cause a 2.5-fold increase in K_i of PepA compared to WT HIV-1p (K_i^{MDR} = 0.23 ± 0.06 μM and Hill slope ∼1.0; K_i^{WT} = 0.094 ± 0.012 μM and Hill slope ∼1.0). Significantly, the MDR mutations do not appear to impact the K_i of compound NIT at all (Figure 3B; K_i^{MDR} = 91 ± 6 μM and Hill slope ∼1.5; K_i^{WT} = 96 ± 3 μM and Hill slope ∼1.6). *The MDR mutant is as sensitive to NIT as the WT.* Furthermore, NIT has a Hill slope value of ∼1.5 in the dose-dependent assay against both WT and MDR HIV-1p. This implies NIT may interact with more than one binding site on the protease, which is consistent with the presence of two Eye sites on each HIV-1p.

Docking of NIT to the Eye site of semiopen HIV-1p with FRED shows that NIT overlays some of the Eye pharmacophores (Figure 3C). The nitro group matches the hydrogen donor pharmacophore, while the isoindoline-1,3-dione (IID) moiety overlaps with the aromatic pharmacophores. In addition, the 4-nitro-IID (4NIID) moiety of compound NIT is similar to the molecular probe, 5NI, which was observed to occupy the Eye site of an apo HIV-1p crystal structure in semiopen conformation.[2] Docking of NIT to the Eye site with FRED generated poses with contacts to HIV-1p similar to 5NI (Figure 3D). The 4NIID moiety forms hydrophobic contacts with Val32, Ile47, Ile54, Pro81, and Ile84 and a hydrogen bond with the amide of Ile50 through the

dx.doi.org/10.1021/jm5008352 | J. Med. Chem. 2014, 57, 6468−6478

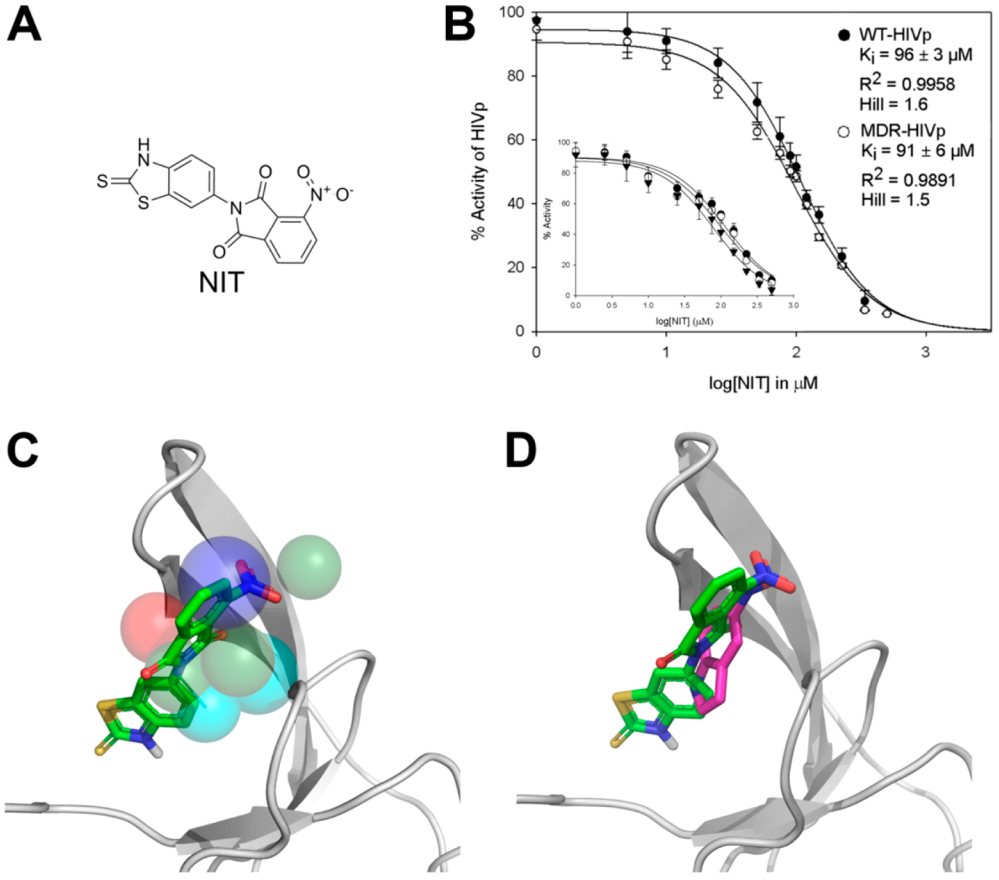

Figure 3. (A) Compound NIT is identified through Markush chemical similarity search queries built from compound **1**. (B) Dose-dependence inhibition curves of compound NIT against HIV-1p. It has similar inhibitory activity against the WT (●, K_i = 96 ± 3 μM) and MDR HIV-1p (○, K_i = 92 ± 6 μM) at 30 nM protease concentration. The insert figure is the dose-dependence inhibition curves of NIT at different WT HIV-1p concentrations (▼, 15 nM; ○, 30 nM; ●, 45 nM) and have very similar Hill slope values. (C) FRED[66] docking pose of NIT (green stick) overlaying with the Eye site pharmacophore model.[1] The pharmacophores are color-coded according to chemical property: hydrophobic (cyan), aromatic (green), hydrogen-bond donor (red), and hydrogen-bond acceptor (blue). (D) FRED docking pose of NIT (green stick) overlaying with the crystal fragment 5NI (purple stick) in the Eye site.[2]

nitro group, similar to the interactions seen in the 5NI–protease complex crystal structure. The benzothiazole-2-thione moiety of NIT forms hydrophobic contacts with Val32, Ile47, and Leu76 and hydrogen bonds with Asp30 and Gly48. These additional interactions likely explain the slight difference in orientation of the 4NIID moiety of compound NIT, relative to the posing of 5NI in the crystal structure (Figure 3D).

NIT Affects Michaelis–Menten Kinetics. To determine the effect of compound NIT on the kinetics of the HIV-1p, we determined the protease activity at various substrate concentrations (2.5–100 μM) using several concentrations of NIT. We obtained the K_m and V_{max} parameters of the HIV-1p through fitting the measured initial velocities to the Michaelis–Menten kinetics model using nonlinear, least-squares regression. We observed dose-dependent changes in the K_m and V_{max} of WT HIV-1p after the introduction of NIT. The result is consistent with mixed competitive inhibition kinetics, where the apparent K_m increases as NIT concentration increases, while V_{max} decreases concurrently (Table 1). The same trend is also observed in the MDR HIV-1p. This suggests NIT may be able to bind to both apo and substrate-bound HIV-1p and may bind to an allosteric site as a mixed competitive inhibitor rather than binding to the catalytic site as a competitive inhibitor.

Ruling Out NIT as Dimerization Inhibitor. Although compound NIT may not act on the HIV-1p through the catalytic site, it is possible that NIT can modulate HIV-1p activity through an alternative site such as the dimer interface. To examine if NIT modulated the observed HIV-1p activity through disrupting the dimer interface, we determined the rate of protease-catalyzed hydrolysis (v_i) of the fluorogenic substrate at various protease concentrations for both WT and MDR strains of HIV-1p, ranging from 0.5 to 30 nM. The resulting initial velocities of the reaction were plotted as $[E]_0/\sqrt{v_i}$ vs $\sqrt{v_i}$ according to the Zhang–Poorman equation. We observed lines with increasing slope as the ligand concentration increased (Figure 4). The same variation in slope was also observed when pepA, a competitive inhibitor, was used as a nondimer inhibitor control (Figure 4; insert). Hence, we determined that NIT does not act as a dimerization inhibitor to HIV-1p as it does not

Table 1. Effects of Compound NIT on the Michaelis–Menten Kinetics of WT and MDR HIV-1p

		compound NIT (μM)		
		0	100	150
WT	V_{max} (nM/s)	44 ± 3	35 ± 3	34 ± 3
	K_m (μM)	91 ± 8	144 ± 18	184 ± 26
MDR	V_{max} (nM/s)	42 ± 6	30 ± 2	30 ± 4
	K_m (μM)	171 ± 36	246 ± 21	359 ± 66

dx.doi.org/10.1021/jm5008352 | J. Med. Chem. 2014, 57, 6468–6478

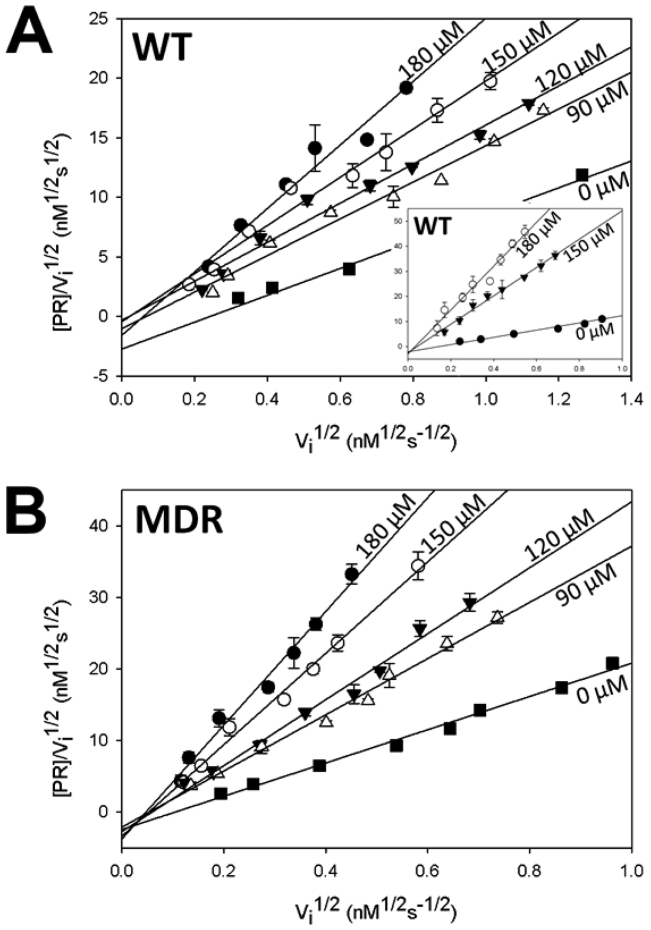

Figure 4. Zhang–Poorman analysis of compound NIT (0.5–30 nM HIV-1p; 5 μM substrate) with (A) WT and (B) MDR HIV-1p. Compound NIT concentrations: ■, 0 μM; Δ, 90 μM; ▼, 120 μM; ○, 150 μM; ●, 180 μM. Nonparallel linear fits of compound NIT at various concentrations indicates the small molecule does not act as a dimerization inhibitor. The small insert in WT shows the Zhang–Poorman plot of PepA, a nondimerization inhibitor (●, 0 nM; ▼, 150 nM; ○, 300 nM).

generate the typical parallel lines seen in classical dimer inhibitors in the Zhang–Poorman plot.[37]

Interaction of NIT and Competitive Inhibitor Pepstatin A. As compound NIT does not affect HIV-1p activity through the dimerization interface and appears as a mixed competitive inhibitor to HIV-1p in the Michaelis–Menten kinetics model, this indicates that NIT can bind to the protease while the substrate is bound to the protease catalytic site. To test how compound NIT interacts with the protease in relation to the substrate, we performed a cross-competitive assay of NIT with PepA. We used the Yonetani–Theorell plot in the form of eq1 to evaluate the binding mode of the small molecule.[42,43,67]

By rearranging eq 1 and plotting the data into eq 2, we obtained factor γ, which represents the degree of mutual influence of the two inhibitors on the binding of each other. In principal, the Yonetani–Theorell plot of v_0/v_i vs $[I_1]$ at various fixed $[I_2]$ will give a series of parallel lines when the two ligands bind to the enzyme in a mutually exclusive manner ($\gamma = \infty$). If the two ligands bind to the enzyme simultaneously, the lines will intercept ($\infty > \gamma > 0$) and the type and strength of mutual interference (facilitation when $0 < \gamma < 1$; hindrance when $1 < \gamma < \infty$) can be assessed by the numerical value of γ. In the case when $\gamma = 1$, the two ligands bind in an independent manner.

$$\frac{v_o}{v_i} = 1 + \frac{[\mathrm{NIT}]}{\mathrm{IC50}_{\mathrm{NIT}}} + \frac{[\mathrm{pepA}]}{\mathrm{IC50}_{\mathrm{pepA}}} + \frac{1}{\gamma}\frac{[\mathrm{NIT}][\mathrm{pepA}]}{\mathrm{IC50}_{\mathrm{NIT}}\mathrm{IC50}_{\mathrm{pepA}}} \quad (1)$$

$$\frac{v_o}{v_i} = \left(1 + \frac{[\mathrm{NIT}]}{\mathrm{IC50}_{\mathrm{NIT}}}\right) + \frac{[\mathrm{pepA}]}{\mathrm{IC50}_{\mathrm{pepA}}}\left(1 + \frac{1}{\gamma}\frac{[\mathrm{NIT}]}{\mathrm{IC50}_{\mathrm{NIT}}}\right) \quad (2)$$

Compound NIT at fixed concentrations was assayed against the competitive inhibitor PepA at various concentrations, and the kinetic data was visualized with the Yonetani–Theorell plot. Intercepting lines of fixed NIT concentration were observed, indicating that NIT does not bind mutually exclusively to the substrate hydrolysis site where PepA binds competitively. NIT yields a γ value that is approximately 1.0 ± 0.2 with both WT and MDR HIV-1p (Figure 5). NIT likely binds independently to a separate site and does not interfere with the binding of competitive inhibitors to the substrate hydrolysis site.

In summary, NIT exhibits mixed inhibition kinetics in the Michaelis–Menten kinetics model, binds independently to a separate site, does not compete with PepA for the substrate

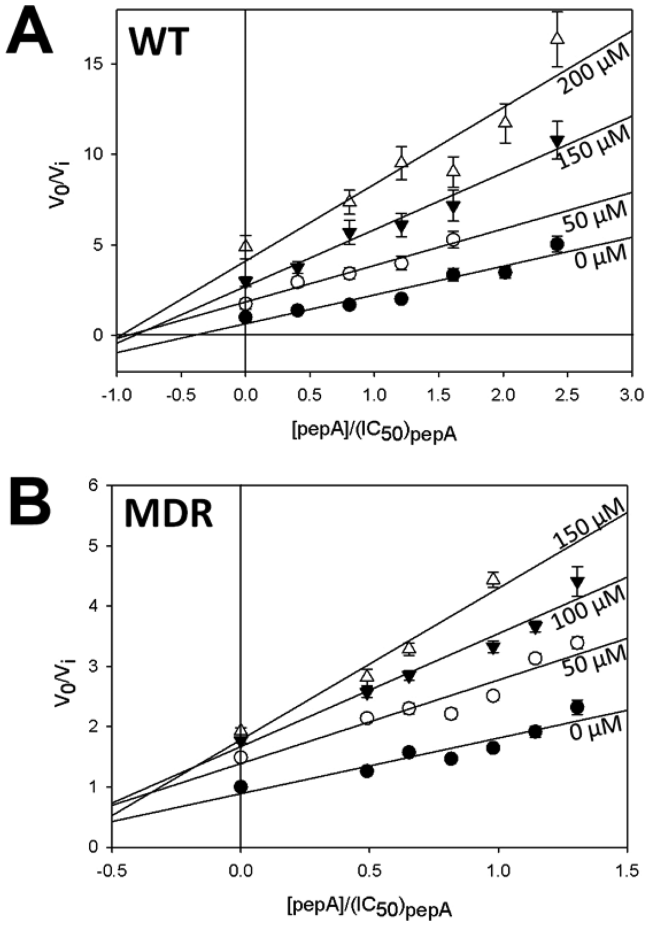

Figure 5. Cross-competitive inhibition analysis of compound NIT (30 nM HIV-1p, 5 μM substrate) against known competitive inhibitor, PepA. (A) WT HIV-1p with compound NIT at concentrations: ●, 0 μM; ○, 90 μM; ▼, 150 μM; and Δ, 200 μM. (B) MDR protease with compound NIT at concentrations: ●, 0 μM; ○, 50 μM; ▼, 100 μM; and Δ, 150 μM. The interaction term γ determined from the curves is approximately 1.0 for both WT and MDR HIV-1p.

dx.doi.org/10.1021/jm5008352 | J. Med. Chem. 2014, 57, 6468–6478

hydrolysis site, and does not modulate HIV-1p activity through the dimerization interface. These kinetics data support the idea that NIT binds to an allosteric site and modulates HIV-1p catalytic activity through a noncompetitive binding mode. Additionally, NIT is topologically similar to compound **1** that fits the MPS pharmacophore,[1] while it is structurally similar to 5NI that overlays to part of the MPS pharmacophore model and is seen crystallographically bound to the Eye site.[2] These data strongly suggest that NIT targets the Eye site of HIV-1p and modulates the protein in a novel allosteric manner. Furthermore, NIT is more attractive chemically because it is more soluble than compound **1** and does not contain an easily cleaved ester linker like **1**. Furthermore, it is equipotent against WT and MDR HIV-1p, which underscores the promise of alternate modes of inhibition to overcome existing clinical resistance.

Dynamics Studies of NIT−Protease Complex. To further examine the interactions between compound NIT and the Eye site of HIV-1p, five independent runs of 20 ns MD simulations were performed (100 ns total). Compound NIT was initially docked into one of the two Eye sites of the homodimeric HIV-1p with Glide, and the docked conformation of NIT with the best score was used as the starting conformation in HIV-1p for simulations. The NIT−protease complex was stable throughout the simulations (see Figure S2A, Figure S2B, and Table S2 in the Supporting Information). During the MD simulations, NIT adjusted its position and remained in the Eye site throughout most of the simulation trajectories. In one of the five trajectories, NIT briefly left the Eye site for 2 ns but returned to the Eye site and remained there for the rest of the trajectory. This rebinding behavior was seen in our previous study of compound **1**.

The median RMSD of NIT throughout the simulation trajectories when compared to the starting frame of the trajectory is 5.1 Å and 50% of the trajectories have RMSD ranging between 3.9 Å to 6.1 Å (Figure S2C, Table S3). NIT remained in the site with a median center-of-mass (COM) distance of 4.7 Å when measuring the distance between all atoms of NIT and the Eye site residues. To put this value in perspective, the COM distance in Figure 3C is 3.6 Å. The COM distance is between 3.3 Å to 5.9 Å in 50% of the analyzed MD trajectories (Figure 6). This demonstrates that NIT binds stably to the Eye site of HIV-1p.

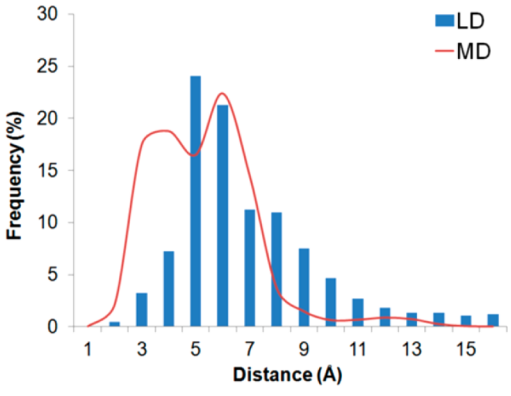

Figure 6. Distribution of distance (Å) between the center-of-mass (COM) of NIT and HIV-1p Eye site in MD and LD simulations. In MD simulations (red line), NIT remained in HIV-1p Eye site throughout all trajectories.

Additionally, five independent runs of 20 ns Langevin dynamics (LD) simulations of the NIT−protease complex were conducted. As there is no dampening effect from the explicit solvent molecules, NIT and HIV-1p alike had more atomic fluctuations compared to the MD simulations (Supporting Information, Figure S3, Table S4). Whereas compound NIT mostly remained in the Eye site of the HIV-1p throughout the trajectory of the MD simulations, NIT in all five independent LD simulations would exit the Eye site, sample conformations along the protein surface, and rebind to one of the 2 Eye sites of HIV-1p (Figure 7). Two possible paths of NIT transition

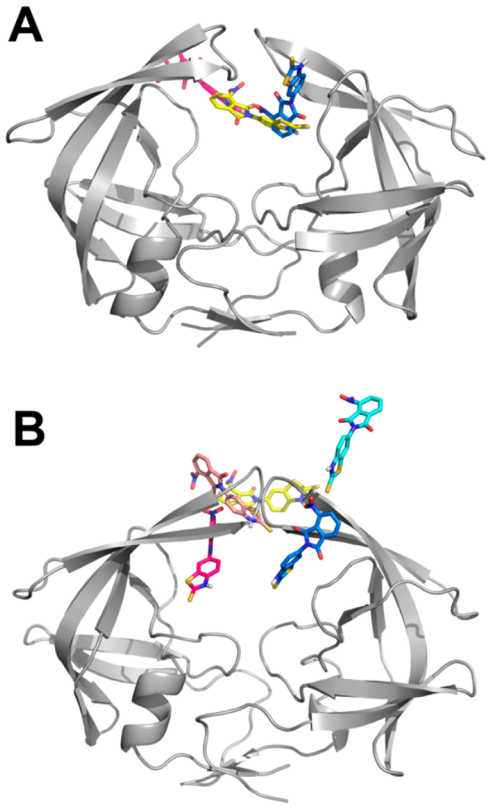

Figure 7. Paths of NIT transition between two Eye sites of HIV-1p. (A) NIT traveled across the active site from one Eye site to the other without complete dissociation from the protease. (B) NIT dissociates from one Eye site and travels along to surface of the flaps before binding to the opposite Eye site.

from one Eye site to another are observed; one path moves along across the active site without full dissociating from the HIV-1p as seen previously in Damm et al.[1] The other path involves a full exit of the HIV-1p, sampling the surface of the flaps and rebinding the Eye site on the opposite monomer (Figure 7B). This indicates that NIT is able to sample both of the available Eye sites. Overall, compound NIT is within the monomer 1's Eye site during ~40% of the trajectories at 7.0 Å COM distance cutoff and within the monomer 2's Eye site ~28% at 7.0 Å COM distance cutoff. Combined, at a 7.0 Å COM distance cutoff, NIT occupied Eye sites in HIV-1p monomer 1 or 2 during ~68% of the trajectory. The remaining time, it mostly sampled along the surface of the flap region. The COM distance ranged between 4.7 and 7.7 Å and a median distance of 5.6 Å for 50% of the analyzed trajectories. The high frequency of sampling at the Eye sites demonstrates that it is viable for ligand binding (Figure 6).

dx.doi.org/10.1021/jm5008352 | J. Med. Chem. 2014, 57, 6468−6478

Throughout the MD trajectories, NIT interacted primarily (>50% of the trajectory) with the flap residues (Ile47, Gly48, Gly49, Ile50, Ile54) and with the bottom of the Eye site (Val32, Gly78, Pro79, Thr80, Pro81, Ile84). These residues were frequently with a heavy-atom cutoff distance of 4.1 Å (Figure 8). Of the residues that NIT consistently interacted with,

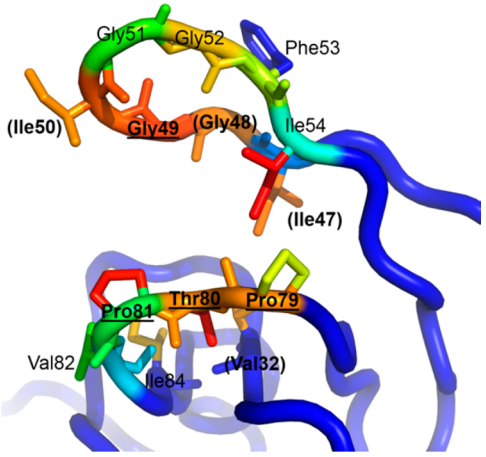

Figure 8. HIV-1p residues in contact with compound NIT. Residues with over 30% of the trajectory in contact with NIT (heavy-atom cutoff distance 4.1 Å) during MD simulations are colored, where blue is below the threshold 30% and red is the maximum 80% of the simulations. Bolded and underlined residues are found to be highly conserved, and those with name in bold and bracket are found to have conservative mutations in the clinic.

Gly49, Gly78, Pro79, Thr80, and Pro81 are known to be highly conserved;[68,69] most importantly, Thr80 has such a strong influence on the flap region's flexibility that a mutation of this invariant residue results in a deleterious effect on HIV-1p catalytic activity.[38] Four residues that NIT interacts with are known to have conservative mutations that maintain the hydrophobic nature of the side chains: Val32(I), Ile47(V/A), Gly48(V), and Ile50(V/L).[68,69] Ile54 and Ile84, which have relatively low frequency of contact with the ligand (Figure 8), are known to have nonconservative mutations although the most common clinically observed mutations maintain the hydrophobic character of the side chain: Ile54(V) and Ile84(V/A).

To examine the change in the dynamic behaviors of HIV-1p due to the binding of NIT to the Eye site, essential dynamics analysis was applied to analyze the MD trajectories of NIT−protease complex and an apo protease. Essential dynamics analyzes the protein dynamics by performing an orthogonal transformation of a covariance matrix of the MD trajectories and isolates the collective modes of motion of the protein. An individual mode of motion, or eigenvector, contains the collective motion of the residues of the examined protein while the associating eigenvalue quantifies the contribution of the eigenvector in the examined trajectories. Each of these eigenvectors can be visualized and inspected separately to distinguish the main modes of collective motion from the more localized fluctuations. The first few eigenvectors, or modes of motion, usually describe the global, dynamic motions of the protein (i.e., domain movement and change in protein conformation), while the higher-order modes of motion usually describe the local dynamic motions (i.e., residue side chain movements).

To compare the essential dynamics of NIT−protease complex to apo-protease, a dot-product was calculated between the eigenvectors as a measurement of the degree of overlap between the examined vectors. Visual inspection of the MD and comparison of the first eigenvector of both systems, as shown in Figure 9, indicates a significant conformational change to the

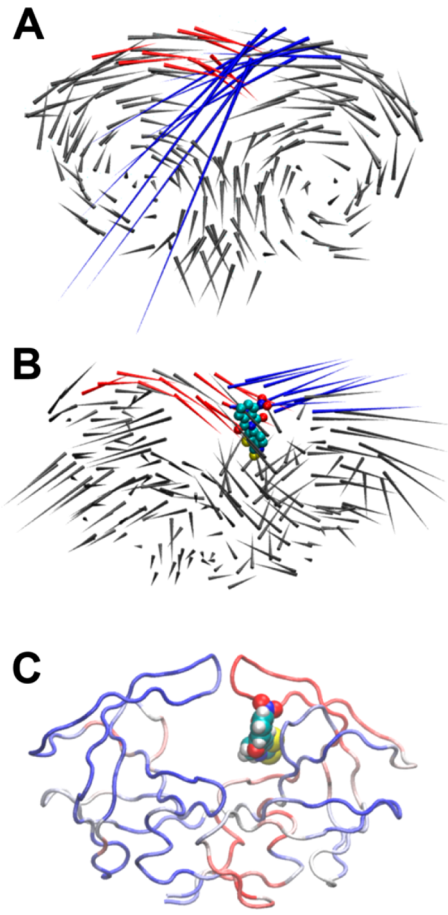

Figure 9. ED indicates how the binding of NIT influences HIV-1p flap movement. The first eigenvector of the ED of (A) apo HIV-1p MD simulation and (B) NIT−protease MD simulations indicates the most significant motions of the protease. Vectors of the flap residue are colored: monomer A is in red and monomer B is in blue. The presence of NIT in the Eye site induces significant localized change in flap movements. (C) Quantitative comparison of the eigenvectors is done through the calculation of the dot-product of (A) and (B). In this last frame, the blue color indicates strong correlation while red color indicates strong anticorrelation for residue motion in the two eigenvectors.

flap in contact with NIT, for which the motion of the flap in NIT−protease complex and in apo protease is strongly anticorrelated (the rest of the protein remains relatively correlated). Furthermore, both first eigenvectors have significant contribution to the overall dynamic motion of the protease in each respective trajectory; the first eigenvector of NIT−protease complex has a normalized eigenvalue of 0.403, while apo-protease has a normalized eigenvalue of 0.540. This strongly suggests that the influence of the extensive interactions with compound NIT in the Eye site has a profound effect on the dynamic motion the flap throughout the trajectory, as one might expect.

dx.doi.org/10.1021/jm5008352 | J. Med. Chem. 2014, 57, 6468−6478

Another observation is the change in the flap openness of HIV-1p in the MD trajectories through binding of NIT to the Eye site (Table 2). The degree of flap openness can be described by the C_α distance measured between catalytic Asp25 and flap-tip Ile50.[70] The flap-opening distance in 50% of the trajectories ranges between 13.7 and 15.8 Å with a median of 14.8 Å, and the opposite monomer with no NIT bound to the Eye site has a similar flap opening distance between 13.0 and 16.1 Å with a median of 14.3 Å (Table 2). This is compared to the apo HIV-1p MD trajectory where 50% of the trajectory has a flap opening distance of 11.9−17.3 Å and a median of 15.1 Å. The flaps under the influence of NIT remain in the semiopen conformation states comparable to the semiopen conformational states observed in apo HIV-1p (median of 14.8 Å with NIT and 14.3 Å without NIT vs 15.1 Å in apo HIV-1p) and has a smaller range of motion compared to the apo HIV-1p (RMS distance ∼2.7 Å for NIT−protease complex vs ∼3.8 Å for apo HIV-1p).

Table 2. Distribution of Flap Openness and Width of Eye Site of NIT−Protease MD Simulations, Shown in Percentiles of the Population Similar to Box Plots

	flap openness (Asp25 C_α−Ile50 C_α) (Å)				
	2.5%	25.0%	50.0%	75.0%	97.5%
A (NIT)	11.0	13.7	14.8	15.8	24.4
B (none)	11.4	13.0	14.3	16.1	20.1
apo	10.0	11.9	15.1	17.3	25.7
	Eye site width (Gly51 C_α−Thr80 C_α) (Å)				
	2.5%	25.0%	50.0%	75.0%	97.5%
A (NIT)	8.8	11.3	12.8	14.4	17.6
B (none)	8.6	10.6	12.1	13.6	15.6
apo	4.7	8.4	9.7	11.9	17.0

We also observed a change in the width of the Eye site relative to the apo HIV-1p, which can be measured by the C_α distance between Gly51 and Thr80 (Table 2). In the NIT−protease complex simulations, the Eye site with NIT bound has a width that ranges between 11.3 and 14.4 Å and a median width of 12.8 Å, while the opposite Eye site with no bound NIT has width between 10.6 and 13.6 Å and a median of 12.1 Å. The two Eye sites of the apo HIV-1p MD trajectory have a similar width distribution that ranges between 8.4 and 11.9 Å and a median width of 9.7 Å. As such, the width of the Eye site in the NIT−protease complex simulations is notably larger than the Eye site in the apo HIV-1p simulation (median of 12.8 Å with NIT and 12.1 Å without NIT vs 9.7 Å in apo HIV-1p). This demonstrates that the presence of NIT affects the flap mobility and flap conformation through its binding to the Eye site.

CONCLUSION

We have described the discovery of a novel small molecule that likely probes the allosteric Eye site of HIV-1p. Compound NIT, with a novel scaffold, demonstrates an allosteric mechanism in modulating the HIV-1p proteolytic activity. It has a mixed competitive inhibition character in the Michaelis−Menten enzymatic kinetics, demonstrating its potential to act on the HIV-1p through a mechanism other than competing for the active site. It is likely that NIT modulates HIV-1p proteolytic activity through the allosteric Eye site of the protease, as shown in the Yonetani−Theorell experiment. MD simulations of a NIT−protease complex show that NIT remains stably bound in the Eye site and affects the dynamics of the β-hairpin flaps when compared to an apo HIV-1p simulation. Moreover, compound NIT has chemical features and binding modes that closely resemble compound 5NI bound in the Eye site, as seen by crystallography.

These data support compound NIT's ability to allosterically modulate HIV-1p proteolytic activity through binding to the Eye site of HIV-1p and altering its dynamics. Most importantly, this new inhibitor is equipotent against WT and MDR HIV-1p. This new mode of inhibition has the promise of overcoming existing clinical resistance, and we believe this is the first small, drug-like molecule reported to do so.

ASSOCIATED CONTENT

Supporting Information

List of all purchased compounds and their activities, RMSD of protease and NIT over the course of the MD and LD simulations, atomic fluctuations over the dynamics simulations, MS and NMR data for NIT. This material is available free of charge via the Internet at http://pubs.acs.org.

AUTHOR INFORMATION

Corresponding Author

*Phone: 734-615-6841. Fax: 734-763-2022. E-mail: carlsonh@umich.edu.

Notes

The authors declare no competing financial interest.

ACKNOWLEDGMENTS

This work has been supported by the National Institutes of Health (GM65372). We thank Dr. C. David Stout and Dr. Alex Perryman for helpful discussions and sharing the crystal structure of 5-nitroindole bound HIV-1 protease. We thank Dr. Celia Schiffer for her generous donation of WT and MDR HIV-1p. We thank Dr. Charles L. Brooks, III, for providing access to the Gollum cluster at the University of Michigan. We greatly appreciate the generous donation of the EON, FILTER, FRED, OMEGA, and ROCS software from OpenEye, Inc. PM-UU is grateful for receiving fellowships from Fred W. Lyons and the University of Michigan Regents.

ABBREVIATIONS USED

4NIID, 4-nitro-isoindoline-1,3-dione; 5NI, 5-nitroindole; CCG, Center for Chemical Genomics; COM, center-of-mass; ED, essential dynamics; EPR, electron paramagnetic resonance; HIV-1p, human immunodeficiency virus type-1 protease; IID, isoindoline-1,3-dione; K_m, Michaelis constant; LD, Langevin dynamics; MD, molecular dynamics; MDR, multidrug resistant; MPS, multiple protein structure; NIT, 4-nitro-2-(2-thioxo-2,3-dihydrobenzothiazol-6-yl)isoindoline-1,3-dione; NMR, nuclear magnetic resonance; PepA, pepstatin A; RMSD, root-mean-square deviation; WT, wild type

REFERENCES

(1) Damm, K. L.; Ung, P. M.-U.; Quintero, J. J.; Gestwicki, J. E.; Carlson, H. A. A Poke in the Eye: Inhibiting HIV-1 Protease through Its Flap-Recognition Pocket. *Biopolymers* **2008**, *89*, 643−652.

(2) Perryman, A. L.; Zhang, Q.; Soutter, H. H.; Rosenfeld, R.; McRee, D. E.; Olsen, A. J.; Elder, J. E.; Stout, C. D. Fragment-Based Screen Against HIV Protease. *Chem. Biol. Drug Des.* **2010**, *75*, 257−268.

(3) Frauenfelder, H.; Sligar, S. G.; Wolynes, P. G. The Energy Landscape and Motions of Proteins. *Science* **1991**, *254*, 1598−1603.
(4) Boehr, D. D.; Nussinov, R.; Wright, P. E. The Role of Dynamic Conformational Ensembles in Biomolecular Recognition. *Nature Chem. Biol.* **2009**, *5*, 789−796.
(5) Kroeger Smith, M. B.; Rouzer, C. A.; Taneyhill, L. A.; Smith, N. A.; Hughes, S. H.; Boyer, P. L.; Janssen, P. A. J.; Moereels, H.; Koymans, L.; Arnold, E.; Ding, J.; Das, K.; Zhang, W.; Michejda, C. J.; Smith, R. H. Molecular Modeling Studies of HIV-1 Reverse Transcriptase Nonnucleoside Inhibitors: Total Energy of Complexation as a Predictor of Drug Placement and Activity. *Protein Sci.* **1995**, *4*, 2203−2222.
(6) Carlson, H. A. Protein Flexibility and Drug Design: How to Hit a Moving Target. *Curr. Opin. Chem. Biol.* **2002**, *6*, 447−452.
(7) Carlson, H. A. Protein Flexibility is an Important Component of Structure-Based Drug Discovery. *Curr. Pharm. Des.* **2002**, *8*, 1571−1578.
(8) Teague, S. J. Implications of Protein Flexibility for Drug Discovery. *Nature Rev. Drug Discovery* **2003**, *2*, 527−541.
(9) Kohl, N. E.; Emini, E. A.; Schleif, W. A.; Davis, L. J.; Heimbach, J. C.; Dixon, R. A.; Scolnick, E. M.; Sigal, I. S. Active Human Immunodeficiency Virus Protease is Required for Viral Infectivity. *Proc. Natl. Acad. Sci. U. S. A.* **1988**, *85*, 4686−4690.
(10) Flexner, C. HIV Drug Development: the Next 25 Years. *Nature Rev. Drug Discovery* **2007**, *6*, 959−966.
(11) Wlodawer, A.; Miller, M.; Jaskólski, M.; Sathyanarayana, B. K.; Baldwin, E.; Weber, I. T.; Selk, L. M.; Clawson, L.; Schneider, J.; Kent, S. B. H. Conserved Folding in Retroviral Proteases: Crystal Structure of a Synthetic HIV-1 Protease. *Science* **1989**, *245*, 616−621.
(12) Prabu-Jeyabalan, M.; King, N. M.; Nalivaika, E. A.; Heilek-Snyder, G.; Cammack, N.; Schiffer, C. A. Substrate Envelope and Drug Resistance: Crystal Structure of Ro1 in Complex with Wild-Type Human Immunodeficiency Virus Type 1 Protease. *Antimicrob. Agents Chemother.* **2006**, *50*, 1518−1521.
(13) Ding, F.; Layten, M.; Simmerling, C. Solution Structure of HIV-1 Protease Flaps Probed by Comparison of Molecular Dynamics Simulation Ensembles and EPR Experiments. *J. Am. Chem. Soc.* **2008**, *130*, 7184−7185.
(14) Galiano, L.; Ding, F.; Veloro, A. M.; Blackburn, M. E.; Simmerling, C.; Fanucci, G. E. Drug Pressure Selected Mutations in HIV-1 Protease Alter Flap Conformations. *J. Am. Chem. Soc.* **2009**, *131*, 430−431.
(15) Ishima, R.; Louis, J. M. A Diverse View of Protein Dynamics from NMR Studies of HIV-1 Protease Flaps. *Proteins* **2008**, *70*, 1408−1415.
(16) Perryman, A. L.; Lin, J.-H.; McCammon, J. A. Restrained Molecular Dynamics Simulations of HIV-1 Protease: The First Step in Validating a New Target for Drug Design. *Biopolymers* **2006**, *82*, 272−284.
(17) Sadiq, S. K.; De Fabritiis, G. Explicit Solvent Dynamics and Energetics of HIV-1 Protease Flap Opening and Closing. *Proteins* **2010**, *78*, 2873−2885.
(18) Karthik, S.; Senapati, S. Dynamic Flaps in HIV-1 Protease Adopt Unique Ordering at Different Stages in the Catalytic Cycle. *Proteins* **2011**, *79*, 1830−1840.
(19) Hornak, V.; Okur, A.; Rizzo, R. C.; Simmerling, C. HIV-1 Protease Flaps Spontaneously Open and Reclose in Molecular Dynamics Simulations. *Proc. Natl. Acad. Sci. U. S. A.* **2006**, *103*, 915−920.
(20) Hornak, V.; Okur, A.; Rizzo, R. C.; Simmerling, C. HIV-1 Protease Flaps Spontaneously Close to the Correct Structure in Simulations Following Manual Placement of an Inhibitor into the Open State. *J. Am. Chem. Soc.* **2006**, *128*, 2812−2813.
(21) Hornak, V.; Simmerling, C. Targeting Structural Flexibility in HIV-1 Protease Inhibitor Binding. *Drug Discovery Today* **2007**, *12*, 132−138.
(22) Deng, N.-J.; Zheng, W.; Gallicchio, E.; Levy, R. M. Insights into the Dynamics of HIV-1 Protease: A Kinetic Network Model Constructed from Atomistic Simulations. *J. Am. Chem. Soc.* **2011**, *133*, 9387−9394.
(23) Carlson, H. A.; Masukawa, K. M.; McCammon, J. A. Method for Including the Dynamic Fluctuations of a Protein in Computer-Aided Drug Design. *J. Phys. Chem. A* **1999**, *103*, 10213−10219.
(24) Carlson, H. A.; Masukawa, K. M.; Jorgensen, W. L.; Lins, R. D.; Briggs, J. M.; McCammon, J. A. Developing a Dynamic Pharmacophore Model for HIV-1 Integrase. *J. Med. Chem.* **2000**, *43*, 2100−2114.
(25) Meagher, K. L.; Carlson, H. A. Incorporating Protein Flexibility in Structure-Based Drug Discovery: Using HIV-1 Protease as a Test Case. *J. Am. Chem. Soc.* **2004**, *126*, 13276−13281.
(26) Meagher, K. L.; Lerner, M. G.; Carlson, H. A. Refining the Multiple Protein Structure Pharmacophore Method: Consistency Across Three Independent HIV-1 Protease Models. *J. Med. Chem.* **2006**, *49*, 3478−3484.
(27) Martin, Y. C. 3D Database Searching in Drug Design. *J. Med. Chem.* **1992**, *35*, 2145−2154.
(28) Hurst, T. Flexible 3D Searching: The Directed Tweak Technique. *J. Chem. Inf. Comput. Sci.* **1994**, *34*, 190−196.
(29) *SYBYL*, version 8.0; Tripos International: St. Louis, MO, 2008.
(30) *OMEGA*, version 2.3.2; OpenEye Scientific Software: Santa Fe, NM, 2009.
(31) *EON*, version 2.0.1; OpenEye Scientific Software: Santa Fe, NM, 2009; *ROCS*, version 3.0.0; OpenEye Scientific Software: Santa Fe, NM, 2009.
(32) Matayoshi, E. D.; Wang, G. T.; Krafft, G. A.; Erickson, J. Novel Fluorogenic Substrates for Assaying Retroviral Proteases by Resonance Energy Transfer. *Science* **1990**, *247*, 954−958.
(33) Jordan, S. P.; Zugay, J.; Darke, P. L.; Kuo, L. C. Activity and Dimerization of Human Immunodeficiency Virus Protease as a Function of Solvent Composition and Enzyme Concentration. *J. Biol. Chem.* **1992**, *267*, 20028−20032.
(34) Toth, M. V.; Marshall, G. R. A Simple, Continuous Fluorometric Assay for HIV Protease. *Int. J. Pept. Protein. Res.* **1990**, *36*, 544−550.
(35) Woon, T. C.; Brinkworkth, R. I.; Fairlie, D. P. Inhibition of HIV-1 Proteinase by Metal Ions. *Int. J. Biochem.* **1992**, *24*, 911−914.
(36) York, D. M.; Darden, T. A.; Pedersen, L. G.; Anderson, M. W. Molecular Modeling Studies Suggest that Zinc Ions Inhibit HIV-1 Protease by Binding at Catalytic Aspartates. *Environ. Health Perspect.* **1993**, *101*, 246−250.
(37) Bowman, M. J.; Byrne, S.; Chmielewski, J. Switching between Allosteric and Dimerization Inhibition of HIV-1 Protease. *Chem. Biol.* **2005**, *12*, 439−444.
(38) Foulkes, J. E.; Prabu-Jeyabalan, M.; Cooper, D.; Henderson, G. J.; Harris, J.; Swanstrom, R.; Schiffer, C. A. Role of Invariant Thr80 in Human Immunodeficiency Virus Type 1 Protease Structure, Function, and Viral Infectivity. *J. Virol.* **2006**, *80*, 6906−6916.
(39) Zhang, Z. Y.; Poorman, R. A.; Maggiora, L. L.; Heinrikson, R. L.; Kezdy, F. J. Dissociative Inhibition of Dimeric Enzymes: Kinetic Characterization of the Inhibition of HIV-1 Protease by Its COOH-Terminal Tetrapeptide. *J. Biol. Chem.* **1991**, *266*, 15591−15594.
(40) Schramm, H. J.; Boetzel, J.; Buttner, J.; Fritsche, E.; Gohring, W.; Jaeger, E.; Konig, S.; Thumfart, O.; Wenger, T.; Nagel, N. E.; Schramm, W. The Inhibition of Human Immunodeficiency Virus Protease by 'Interface Peptides'. *Antiviral Res.* **1996**, *30*, 155−170.
(41) Breccia, P.; Boggetto, N.; Perez-Fernandez, R.; Van Gool, M.; Takahashi, M.; Rene, L.; Prados, P.; Badet, B.; Reboud-Ravaux, M.; de Mendoza, J. Dimerization Inhibitors of HIV-1 Protease Based on a Bicyclic Guanidinium Subunit. *J. Med. Chem.* **2003**, *46*, 5196−5207.
(42) Yonetani, T.; Theorell, H. Studies on Liver Alcohol Hydrogenase Complexes. 3. Multiple Inhibition Kinetics in the Presence of Two Competitive Inhibitors. *Arch. Biochem. Biophys.* **1964**, *106*, 243−251.
(43) Martinez-Irujo, J. J.; Villahermosa, M. L.; Mercapide, J.; Cabodevilla, J. F.; Santiago, E. Analysis of the Combined Effect of Two Linear Inhibitors on a Single Enzyme. *Biochem. J.* **1998**, *329*, 689−698.

(44) Chang, M. W.; Giffin, M. J.; Muller, R.; Savage, J.; Lin, Y. C.; Hong, S.; Jin, W.; Whitby, L. R.; Elder, J. H.; Boger, D. L.; Torbett, B. E. Identification of Broad-Based HIV-1 Protease Inhibitors from Combinatorial Libraries. *Biochem. J.* **2010**, *429*, 527−532.
(45) Hornak, V.; Abel, R.; Okur, A.; Strockbine, B.; Roitberg, A.; Simmerling, C. Comparison of Multiple Amber Force Fields and Development of Improved Protein Backbone Parameters. *Proteins* **2006**, *65*, 712−725.
(46) Case, D. A.; Darden, T. A.; Cheatham, T. E., III; Simmerling, C. L.; Wang, J.; Duke, R. E.; Luo, R.; Crowley, M.; Walker, R. C.; Zhang, W.; Merz, K. M.; Wang, B.; Hayik, S.; Roitberg, A.; Seabra, G.; Kolossvary, I.; Wong, K. F.; Paesani, F.; Vanicek, J.; Wu, X.; Brozell, S. R.; Steinbrecher, T.; Gohlke, H.; Yang, L.; Tan, C.; Mongan, J.; Hornak, V.; Cui, G.; Mathews, D. H.; Seetin, M. G.; Sagui, C.; Babin, V.; Kollman, P. A. *AMBER 10*; University of California: San Francisco, 2008.
(47) Spinelli, S.; Liu, Q. Z.; Alzari, P. M.; Hirel, P. H.; Poljak, R. J. The Three-Dimensional Structure of the Aspartyl Protease from the HIV-1 Isolate BRU. *Biochimie* **1991**, *73*, 1391−1396.
(48) Berman, H. M.; Westbrook, J.; Feng, Z.; Gilliland, G.; Bhat, T. N.; Weissig, H.; Shindyalov, I. N.; Bourne, P. E. The Protein Data Bank. *Nucleic Acids Res.* **2000**, *28*, 235−242.
(49) *PyMOL Molecular Graphics System*, version 1.2; Schrödinger, LLC: New York.
(50) *Glide*, version 5.5; Schrödinger, LLC: New York, 2009.
(51) Dupradeau, F.-Y.; Pigache, A.; Zaffran, T.; Savineau, C.; Lelong, R.; Grivel, N.; Lelong, D.; Rosanski, W.; Cieplak, P. The R.E.D. Tools: Advances in RESP and ESP Charge Derivation and Force Field Library Building. *Phys. Chem. Chem. Phys.* **2010**, *12*, 7821−7839.
(52) Wang, J.; Wolf, R. M.; Caldwell, J. W.; Kollman, P. A.; Case, D. A. Development and Testing of a General Amber Force Field. *J. Comput. Chem.* **2004**, *25*, 1157−1174.
(53) Wang, J.; Wang, W.; Kollman, P. A.; Case, D. A. Automatic Atom Type and Bond Type Perception in Molecular Mechanical Calculations. *J. Mol. Graphics Modell.* **2006**, *25*, 247−260.
(54) Jorgensen, W. L.; Chandrasekhar, J.; Madura, J. D.; Impey, R. W.; Klein, M. L. Comparison of Simple Potential Functions for Simulating Liquid Water. *J. Chem. Phys.* **1983**, *79*, 926−935.
(55) Darden, T. A.; York, D. M.; Pedersen, L. G. Particle Mesh Ewald. An N.log(N) Method for Ewald Sums in Large Systems. *J. Chem. Phys.* **1993**, *98*, 10089−10092.
(56) Ryckaert, J. P.; Ciccotti, G.; Berendsen, H. J. C. Numerical Integration of the Cartesian Equations of Motion of a System with Constraints: Molecular Dynamics of *n*-Alkanes. *J. Comput. Phys.* **1977**, *23*, 327−341.
(57) Meagher, K. L.; Carlson, H. A. Solvation Influences Flap Collapsein HIV-1 Protease. *Proteins* **2005**, *58*, 119−125.
(58) Still, W. C.; Tempczyk, A.; Hawley, R. C.; Hendrickson, T. Semianalytical Treatment of Salvation for Molecular Mechanics and Dynamics. *J. Am. Chem. Soc.* **1990**, *112*, 6127−6129.
(59) García, A. E. Large-Amplitude Nonlinear Motions in Proteins. *Phys. Rev. Lett.* **1992**, *68*, 2696−2699.
(60) Amadei, A.; Linssen, A. B. M.; Berendsen, H. J. C. Essential Dynamics of Proteins. *Proteins* **1993**, *17*, 412−425.
(61) Mongan, J. Interactive Essential Dynamics. *J. Comput.-Aided Mol. Des.* **2004**, *18*, 433−436.
(62) Humphrey, W.; Dalke, A.; Schulten, K. VMD—Visual Molecular Dynamics. *J. Mol. Graphics* **1996**, *14*, 33−38.
(63) *FILTER*; OpenEye Scientific Software: Santa Fe, NM, 2012.
(64) Baell, J. B.; Holloway, G. A. New Substructure Filters for Removal of Pan Assay Interference Compounds [PAINS] from Screening Libraries and for their Exclusion in Bioassays. *J. Med. Chem.* **2010**, *53*, 2719−2740.
(65) Shoichet, B. K. Interpreting Steep Dose-Response Curves in Early Inhibitor Discovery. *J. Med. Chem.* **2006**, *49*, 7274−7277.
(66) *FRED*, version 2.2.5; OpenEye Scientific Software: Santa Fe, NM, 2009.
(67) Asante-Appiah, E.; Chan, W. W. Analysis of the Interactions between an Enzyme and Multiple Inhibitors using Combination Plots. *Biochem. J.* **1996**, *320*, 17−26.
(68) Shafer, R. W.; Rhee, S. Y.; Pillay, D.; Miller, V.; Sandstrom, P.; Schapiro, J. M.; Kuritzkes, D. R.; Bennett, D. HIV-1 Protease and Reverse Transcriptase Mutations for Drug Resistance Surveillance. *AIDS* **2007**, *21*, 215−223.
(69) Johnson, V. A.; Brun-Vézinet, F.; Clotet, B.; Günthard, H. F.; Juritzkes, D. R.; Pillay, D.; Schapiro, J. M.; Richman, D. D. Update of the Drug Resistance Mutations in HIV-1: December 2010. *Top. HIV Med.* **2010**, *18*, 156−163.
(70) Perryman, A. L.; Lin, J.-H.; McCammon, J. A. HIV-1 Protease Molecular Dynamics of a Wild-Type and of the V82F/I84V Mutant: Possible Contributions to Drug Resistance and a Potential New Target Site for Drugs. *Protein Sci.* **2004**, *13*, 1108−1123.